Energy-based Considerations for Ungrounded Wearable UHF Antenna Design

Giovanni Andrea Casula, *Member, IEEE,* Andrea Michel, *Member, IEEE,* Giorgio Montisci, *Member, IEEE,* Paolo Nepa, *Member, IEEE,* Giuseppe Valente

***Abstract*—The robustness of wearable UHF-band ungrounded antennas with respect to body-coupling effects is addressed. Two different configurations of single-layer antennas, with different energy density distributions, are presented, and a design criterion to improve their performance with respect to the antenna-body separation is derived. Through an analysis of the antenna electric and magnetic energy density distributions, it is shown that the degradation of the antenna performance due to the proximity of the human body can be reduced if the electric energy density is confined in specific regions far from the antenna border. The proposed design criterion has been validated by numerical simulations and experimental measurements.**

***Index Terms*—Wearable antennas, body-antenna coupling, ungrounded antennas.**

I. INTRODUCTION

IT is well known that the performance of wearable antennas is significantly modified by the human body proximity [1]-[2]. Compared with the stand-alone antenna, the coupling between the antenna and the human body modifies the antenna input impedance, causes antenna detuning, and it is responsible for the antenna radiation efficiency degradation and the radiation pattern fragmentation. All these effects are strictly related to the antenna size, layout, and operating frequency [1]. At the UHF band, antennas with a size between $\lambda/5$ and $\lambda/2$ (λ being the free-space wavelength) are quite common, since they allow for the realization of a relatively efficient wearable antenna that can still be made unobtrusive and comfortable to the user. A large number of scientific papers are explicitly devoted to the analysis of the effects of the antenna-body coupling on the antenna performance, and to the evaluation of the power absorption of the biological tissues (the latter being quantified through the SAR parameter – Specific Absorption Rate). However, in real-world applications, the antenna-body distance can change in a random way, due to the wearer natural movements [3]-[5]. Moreover, the electromagnetic and geometrical parameters of the antenna platform (namely, the human body) change from person to person, as well as for different locations of the antenna on the same person, since such parameters vary around the body [6]. The antenna parameters modification due to the above random effects can determine a significant and uncontrolled degradation of the radio link. Therefore, specific design criteria are required to enhance the robustness of the antenna performance with respect to the variation of the human body distance and of its dielectric characteristics.

In a number of papers [7]-[8], it has been shown that electrically small *magnetic* antennas can perform better than electrically small *electric* antennas when they operate close to, or inside, the human body (or any other non-magnetic lossy material). It is worth noting that, in electrically small antennas (either electric or magnetic antennas), only one of the two energy densities dominates in the near-field (NF) region (e.g., the magnetic energy density for the small loop antenna and its variants). On the other hand, most of the UHF wearable antennas have a size between $\lambda/5$ and $\lambda/2$, so they can exhibit one or more maxima of the electric and magnetic energy densities in their NF region.

Recently, in order to enhance the robustness of UHF grounded wearable printed antennas with respect to the antenna-body coupling effects, the authors proposed a criterion for the choice of the optimal shape and size of the antenna ground plane [9]-[11]. In particular, the optimal ground plane shape has been related to the position of the maxima of the electric and magnetic energy densities, in order to hinder impedance detuning and efficiency reduction.

However, the physical structure of antennas with a ground plane printed on the back side of the dielectric layer (referred as "grounded antennas" [9]-[11]), could limit the mechanical flexibility, which is an important feature of wearable antennas. As a matter of fact, these antennas should be unobtrusive and comfortable, but the use of a large ground plane could be in contrast with these requirements. As an alternative, wearable antennas without the ground plane [12] (denoted in the following as "ungrounded" antennas) can be used. These antennas can be directly integrated in existing clothes, also thanks to the recent advances in textile antennas design, and fabrication of circuits with intricate details [13]-[15]. However, the absence of a metallic ground plane makes these antennas more sensitive to the human body proximity effect. Thus, increasing their robustness with respect to the antenna-body coupling effects is an important challenge for the antenna designer. Therefore, in this paper, an energy-based design criterion for ungrounded printed wearable antennas is suggested, aimed to improve their robustness with respect to the distance from the human body. The design guidelines presented in [9] for grounded antennas lead to an enlargement of the ground plane in the direction of the maxima of the electric energy density. However, the latter strategy cannot be applied to ungrounded antennas, and a proper discussion is required to derive an energy-based design criterion for such a class of antennas.

In section II, we present simulated results of a resonant circular loop antenna operating in the UHF RFID frequency range (860-960 MHz). This example describes a possible solution capable to increase the ungrounded antennas robustness, and helps us to introduce an energy-based design criterion for these antennas. In particular, based on the antenna electric and magnetic energy density distributions, a layout modification has been introduced [16]-[17], aiming to confine the electric energy density in specific regions far from the antenna border, thus increasing the insulating capability of the dielectric substrate.

In order to validate the proposed design criterion, we investigate the robustness with respect to the human body coupling of a second antenna, selected from the open literature, namely the nested-slot suspended-patch (NSSP) antenna operating at 870 MHz, whose performance is assessed and experimentally tested in [12]. Then, we have suitably modified the initial layout of [12] in order to confine the electric energy density far from the antenna border. In this way we are able to single out the effect of the layout modifications to validate our design criterion.

Finally, in section III an experimental assessment is presented. Two prototypes of NSSP antennas have been manufactured in the microwave laboratory of the Cagliari Astronomy Observatory. The measured results are in good agreement with simulations and demonstrate the effectiveness of the proposed design criterion.

II. NUMERICAL SIMULATION RESULTS

In order to describe the proposed energy-based design criterion for ungrounded printed wearable antennas, an isolated (operating in free-space) resonant circular loop antenna (Fig. 1a), printed on a 150 mm × 150 mm, 1 mm thick layer with ε_r = 11.8 and $tan\ \delta$ = 0.00045, has been optimized to resonate at 935 MHz, and the distribution of the electric and magnetic energy densities has been investigated at resonance. Numerical simulations have been performed by using CST Microwave Studio [18].

In Fig. 2, the simulated real and imaginary parts of the antenna input impedance are plotted as a function of the frequency. In Fig. 3a and 3c, the electric and magnetic energy density distributions generated by the antenna in the middle of the substrate are shown. It is worth noting that a strong and almost uniform electric energy density is obtained in proximity of the circular loop, whereas a magnetic null is observed at the position of the loop center. Then, starting from the standard loop antenna, a layout modification has been studied. In particular, the solid microstrip line has been divided into 12 segments, and 0.89 pF lumped capacitors have been introduced between them, but keeping the same radius *R* and width *W* of the loop, and the same layout dimension *L* (see Fig. 1b). The modified configuration (named "segmented loop") is widely used for near-field UHF RFID applications [16]-[17], since it allows to keep the current almost constant and in-phase along the loop, even though the loop perimeter is larger than the operating wavelength. In particular, the presence of the capacitors allows to avoid the current phase-inversion and provides a strong and uniform magnetic field distribution close to the antenna surface. As shown in Fig. 2, the designed segmented loop antenna resonates at the same frequency of the standard resonant loop (935 MHz), whereas the energy density distributions at resonance (Figs. 3b, 3d) are different from those of the resonant loop (Figs. 3a, 3c). Specifically, the magnetic energy density is stronger and more uniform in proximity of the radiating element, and the electric energy is confined within small areas near the lumped capacitors.

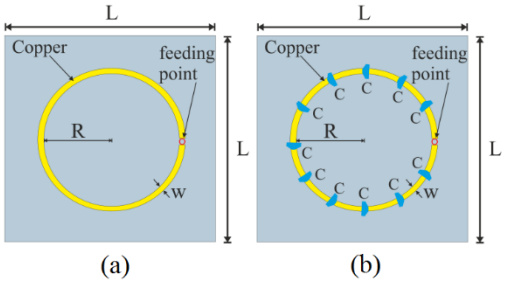

Figure 1. (a) Solid-line resonant loop and (b) segmented loop with lumped capacitors (C = 0.89 pF). The geometrical parameters are: L = 150 mm; R = 50 mm, W = 2.5 mm.

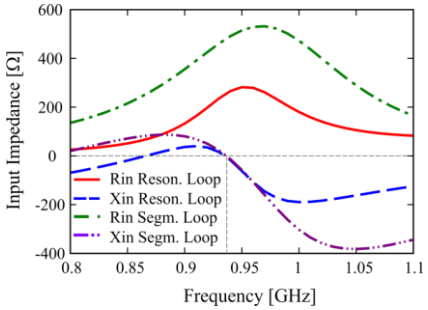

Figure 2. Input impedance of the two loop antennas shown in Fig. 1.

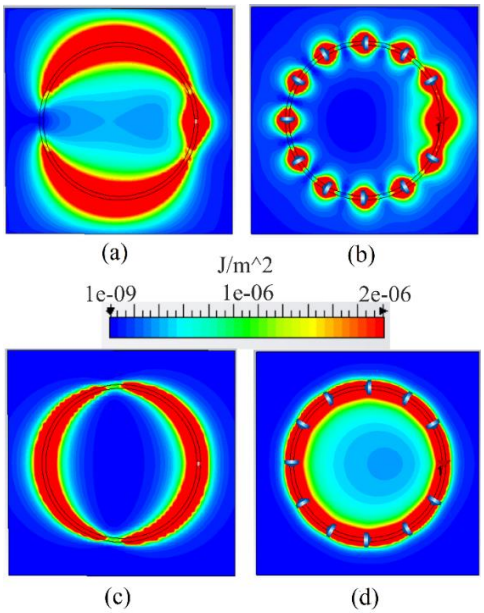

Figure 3. (a) Electric and (c) magnetic energy density distributions of the resonant loop antenna. (b) Electric and (d) magnetic energy density distribution of the segmented loop antenna. All the distributions are computed in the middle of the dielectric substrate at the resonant frequency (935 MHz). The same scale has been used for all the plots.

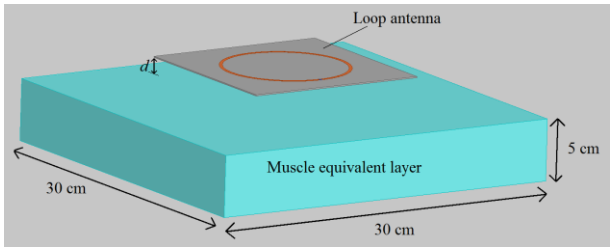

Figure 4. Phantom model used to perform the numerical investigation of the robustness to the body proximity of the loop antennas reported in Fig. 1.

In order to analyze the body-antenna coupling effect on the antenna performance, a numerical phantom has been added to the simulation scenario (see Fig. 4). It is a single-layer equivalent model consisting in a 5-cm-thick material with $\varepsilon_r = 2/3\ \varepsilon_{r\_muscle} = 36$, and $\sigma = 2/3\ \sigma_{muscle} = 0.62$ S/m [19]. The radiation efficiency η and the power transmission coefficient τ have been computed. The latter has been calculated as

$$\tau = 1 - \left|\frac{Z_{IN} - Z_0}{Z_{IN} - Z_0^*}\right|^2 = \frac{4\,\mathrm{Re}(Z_0)\mathrm{Re}(Z_{IN})}{\left|Z_0^* + Z_{IN}\right|^2} \qquad (1)$$

wherein Z_{IN} is the antenna input impedance, and Z_0 is a reference impedance. Since we are interested to analyze the robustness of the different antenna layouts with respect to the variations of the antenna-phantom model separation d (see Fig. 4), Z_0 has been assumed equal to the antenna input impedance at 935 MHz for $d = 0$ mm (*i.e.*, the configuration with the antenna adherent to the body model).

In Fig. 5a, τ is plotted as a function of the distance d, for both the resonant loop and the segmented loop. It should be noted that the power transmission coefficient τ of the segmented loop presents a smaller variation and a higher value than that of the resonant loop. The simulated radiation efficiency of both the antennas is quite small when they are attached to the human body (4 % for the resonant loop, and 9 % for the segmented loop), due to the high losses in the human body tissues. However, it increases when the antenna-body separation increases (Fig. 5(b)).

As a further figure of merit of the robustness of the antenna performance, the product $\tau \times \eta$ is shown in Fig. 5c as a function of d for both the radiating elements, showing an improvement of the segmented loop over the resonant loop.

Since the human tissues are *non-magnetic* materials, it results that a reduction of the sensitivity of the antenna parameters to the body proximity can be achieved by using the segmented loop antenna, which presents a more confined electric density distribution and a stronger magnetic energy density in the dielectric substrate when compared to the resonant loop antenna (see Fig. 3).

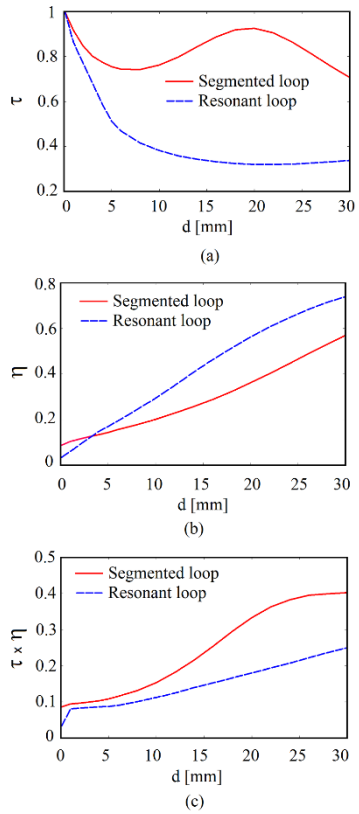

Figure 5. Simulated (a) transmission coefficient τ, (b) radiation efficiency η, and (c) $\tau \times \eta$ as a function of the distance d between the antenna and the phantom, for both the resonant loop and the segmented loop antennas, computed at 935 MHz.

Based on the example presented above, we can conclude that a layout modification aimed to confine the electric energy density in specific regions far from the antenna border may be effective in improving the insulating capability of the dielectric substrate, thus enhancing the antenna robustness with respect to the human body coupling.

In order to validate our design criterion, we consider in the following the single-layer slot antenna for UHF RFID tags proposed in [12], operating at 870 MHz. This antenna is called Nested-Slot Suspended Patch (NSSP), and consists of a H-shaped slot placed onto a suspended patch. The antenna layout is shown in Fig. 6a, and its geometrical parameters are listed in the caption of Fig. 6. This is a versatile layout, because it is capable to match with a large class of microchips by a suitable choice of its geometrical parameters [12].

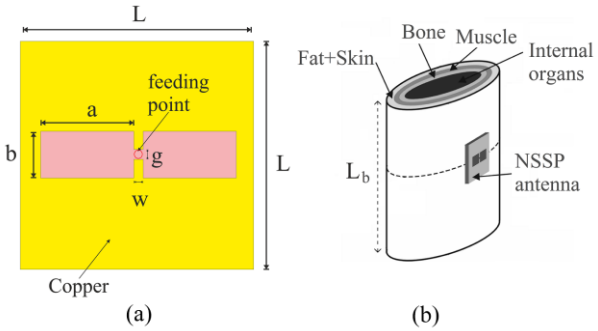

Figure 6. (a) Layout of the RFID tag presented in [12], and (b) antenna placed on a human-body simplified cylindrical model. Geometrical dimensions are: a = 10 mm, b = 20 mm, w = g = 2 mm, L = 50 mm, L_b = 400 mm.

The tag antenna is etched on a rectangular metallic plate printed on a 4-mm-thick silicone dielectric slab (ε_r = 11.8, *tan* δ = 0.00045), which electrically insulates the antenna from the body [12]. To account for the presence of the human body, and to reproduce the performance of the antenna presented in [12], a simplified reference model of the human torso (namely, a stratified elliptical cylinder with physical parameters obtained from the tissue database [12]) has been considered in the simulated environment (Fig. 6b). The reported simulations, performed with CST Microwave Studio, are referred to the case of thick man, which represents the worst case, since the larger absorption of a bigger torso will result in a lower antenna efficiency. The geometrical and physical parameters of the model of the human torso in Fig. 6(b) are reported in Table 1.

Table I. Geometrical and physical parameters of the layered anatomical model in Fig. 6(b) at 870 MHz.

Layer	ε_r	σ [S/m]	Ellipse axes [cm]
Skin + fat	14.5	0.25	50 × 20

Muscle	55.1	0.93	46.5 × 17
Bone	20.8	0.33	42.6 × 12.6
Internal Organs	52.1	0.91	41.0 × 10

The energy density distributions of the antenna, computed in the dielectric substrate, are shown in Fig. 7 for $d = 0$ (antenna attached to the body) at the antenna operating frequency of 870 MHz. It should be noted that peaks of the electric energy density are visible near the antenna center and close to the antenna border along the *y*-axis (Fig. 7a), whereas peaks of magnetic energy density are at the center of the antenna and close to the antenna border along the *x* direction (Fig. 7b).

Then, three configurations have been investigated:

a) ***NSSP*** (the reference layout), which is the reference antenna, as described in [12].
b) ***NSSP-SE***, in which the silicone substrate has been extended toward the regions close to an electric energy density peak (ΔL = 25 mm on both sides), as indicated in Fig. 8a;
c) ***NSSP-SH***, in which the silicone substrate has been extended toward the regions close to a magnetic energy density peak (ΔL = 25 mm on both sides), as indicated in Fig. 8b.

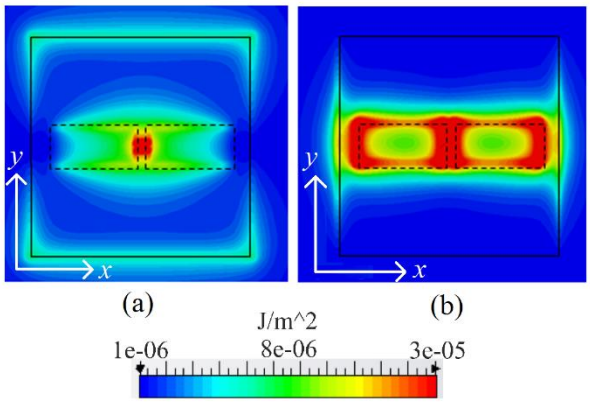

Figure 7. Electric (a) and magnetic (b) energy density distributions of the antenna presented in [12]. The black square represents the antenna contour.

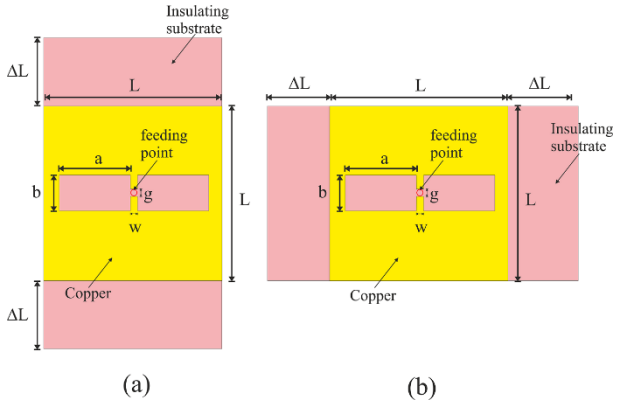

Figure 8. (a) ***NSSP-SE*** and (b) ***NSSP-SH*** configuration layouts.

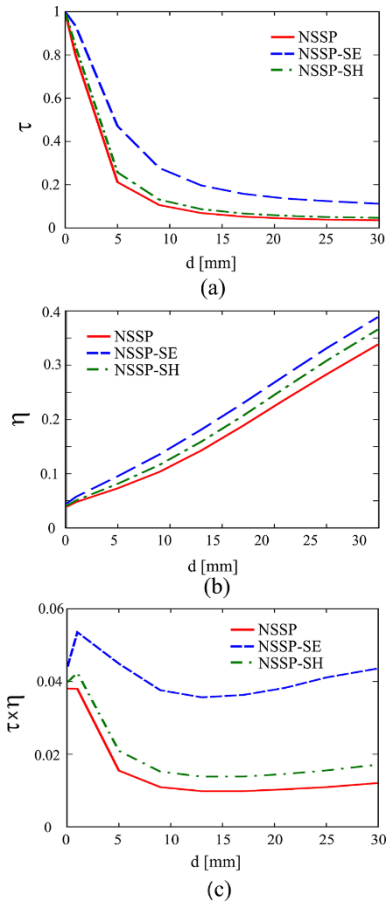

Figure 9. Simulated (a) transmission coefficient τ, (b) radiation efficiency η, and (c) $\tau \times \eta$ as a function of the distance d between the antenna and the phantom, for the NSSP antenna of [12] and its modifications (NSSP-SE and NSSP-SH). Frequency = 870 MHz.

For the above configurations, the behavior of τ, η, and $\tau \times \eta$ as a function of the distance d between the antenna and the body phantom have been investigated, and are shown in Fig. 9. The reference impedance Z_0 in (1) has been assumed equal to the antenna input impedance for d = 0 mm, computed at 870 MHz. As shown in Fig. 9a, the lowest transmission coefficient variation is achieved for the ***NSSP-SE*** configuration. The simulated radiation efficiency is nearly the same for all ***NSSP***, ***NSSP-SE***, and ***NSSP-SH*** configurations: it is about 5% when the antenna is attached to the human body, and around 35%-40% when the antenna is 30 mm far (Fig. 9b). Finally, for the ***NSSP-SE*** configuration, the $\tau \times \eta$ product keeps almost stable against the antenna-body distance (Fig. 9c). In other words, the extension of the insulating silicone substrate toward the regions close to the peaks of the electric energy density improves the robustness of the antenna performance with respect to the human-body coupling.

To further improve the antenna robustness, both the silicone substrate and the metallic plate can be properly extended. Then, we consider also the following configurations:

d) ***NSSP-SME***, in which the layout (both the silicone substrate and the metallization) has been extended toward the regions close to an electric energy density peak (a ΔL = 25 mm extension on both the upper and the lower sides, see Fig. 10a);
e) ***NSSP-SMH***, in which the layout (both the silicone substrate and the metallization) has been extended toward the regions close to a magnetic energy density peak (a ΔL = 25 mm extension on both the right and the left sides, see Fig. 10b);

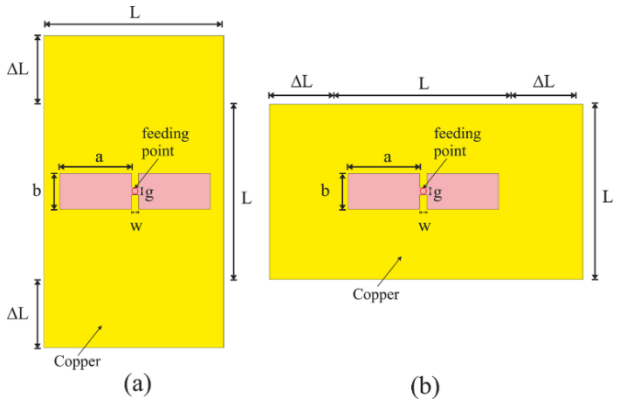

Figure 10. (a) ***NSSP-SME*** and (b) ***NSSP-SMH*** configuration layouts.

The enlargement of the metallic plate does not modify the radiating element (the H-shaped slot), but it may help to shield the antenna from the human body. As shown in Fig. 11, the transmission coefficient of the ***NSSP-SME*** configuration remains quite stable by varying the antenna-body separation (it is greater than 0.7 for a distance d less than 30 mm), whereas the $\tau \times \eta$ rapidly increases with respect to the antenna-body separation. This example clearly demonstrates that an extension of the complete structure (both metallization and silicone substrate) toward the regions close to the peaks of the electric energy density is very effective in improving the robustness of the antenna performance with respect to the human-body coupling.

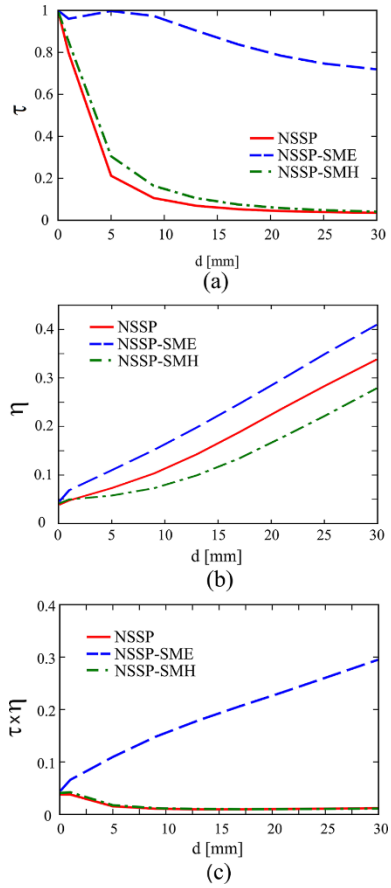

Figure 11. Simulated (a) transmission coefficient τ, (b) radiation efficiency η, and (c) $\tau \times \eta$ as a function of the distance d between the antenna and the phantom, for the NSSP antenna of [12] and its modifications (NSSP-SME and NSSP-SMH). Frequency = 870 MHz.

III. Experimental Validation

The proposed design criterion has been experimentally validated by using prototypes of the NSSP antenna. Specifically, the τ variation has been measured by varying the distance between the antenna and a simplified phantom. As in [12], a monopole-like configuration, consisting of half the NSSP placed vertically over an image plane of aluminum with a coaxial connector in the back side, has been considered (see Figs. 12, 13, and 14).

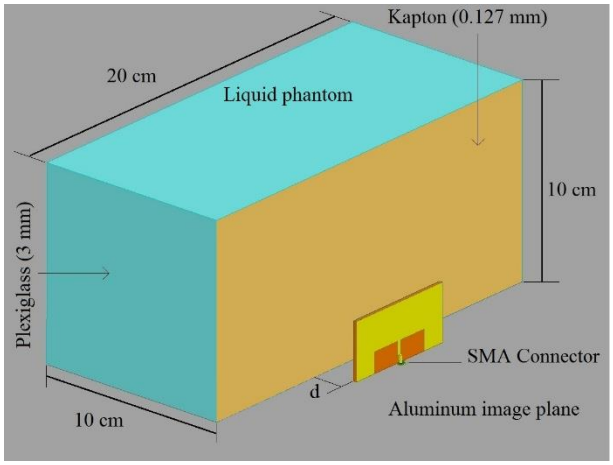

Figure 12. Simulated model of the measurement setup used to investigate the robustness of the NSSP antennas.

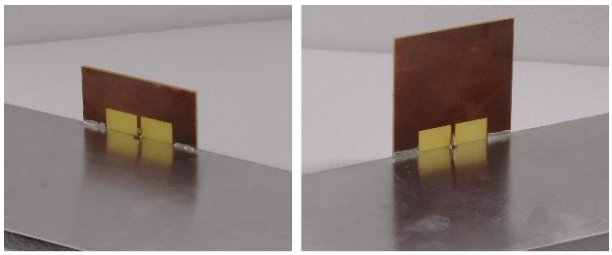

Figure 13. Prototypes of the realized NSSP (left) and NSSP-SME (right) antennas in monopole-like configuration. The feeding coaxial connector is in the back side of the aluminum image plane.

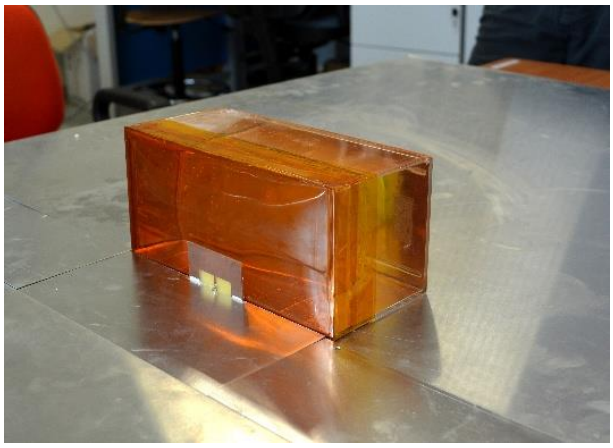

Figure 14. Experimental measurement setup: monopole-like NSSP antenna in front of the liquid phantom.

The antenna prototypes have been realized on a 1.565 mm-thick FR-4 substrate with $\varepsilon_r = 4.4$, and tan $\delta = 0.002$. The human tissue has been experimentally simulated by using a simplified phantom consisting of a box of dimension 20 cm × 10 cm × 10 cm (Figs. 12 and 14). The box is filled up with a tissue-simulating liquid with muscle-like parameters at 870 MHz ($\varepsilon_r = 56.6$, $\sigma = 1.33$ Siemens/m), made with deionized water (53%), saccharose (45.6%) and sodium chloride (1.4%) [20].

In the measurement setup devised in [12], the antenna is a 0.2 mm-thick metallic sheet without dielectric substrate, attached to the external wall of the phantom, a 5 mm-thick Perspex layer, which acts as the layer insulating the antenna from the body [12]. However, in order to evaluate the robustness of the antenna performance with respect to the human-body coupling, our experimental validation requires to vary the distance d of the antenna from the phantom (Fig. 12). In this case, a thick phantom wall would invalidate our analysis, since the insulating layer is part of the antenna, and should be moved together with the antenna, while moving outside the phantom. As a consequence, the face of the phantom behind the antenna has been made as thin as possible using a 127 μm-thick Kapton sheet (with dielectric permittivity 3.5), which has been fixed to a 3 mm-thick plexiglass frame by using kapton adhesive tape and silicone (Figs. 12 and 14).

In order to properly apply the image theory to the liquid phantom, we have covered the internal 20 cm × 10 cm base of the box containing the liquid with 40 μm-thick copper adhesive tape, which is therefore in direct contact with the liquid. Finally, the aluminum sheet with the monopole antenna (see Fig. 13) has been placed at the same level of the copper tape inside the box.

The NSSP antenna under test has been designed to be matched to a $Z_{chip} = 73\text{-}j113\ \Omega$ [21] when it is attached to the body (i.e. for $d = 0$), resulting in the following geometrical dimensions: L = 55 mm, a = 20 mm, b = 15 mm, s = 2 mm (Fig. 6a). A prototype of this antenna in its monopole-like configuration has been manufactured (see Fig. 13 left). To experimentally assess our design criterion a prototype of the NSSP-SME configuration with $\Delta L = 27.5$ mm (see Fig. 13 right) has also been fabricated. Then, the robustness of both the standard NSSP and the NSSP-SME antennas has been evaluated as a function of the distance d between the liquid phantom and the antenna (Figs. 12 and 14).

In Figs. 15 and 16, the simulated and measured input impedance Z_{IN} is reported for the standard NSSP and for the NSSP-SME antennas, respectively. The agreement between simulation and measurement is good. The differences are likely due to the uncertainty in the dielectric properties of the liquid phantom.

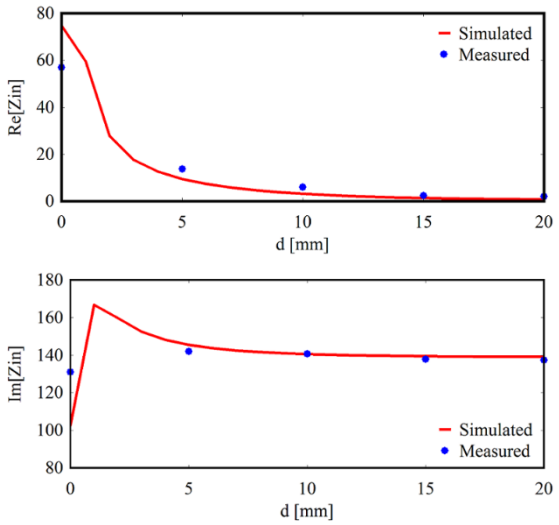

Figure 15. Simulated and measured input impedance of the NSSP antenna in Fig. 13 (left).

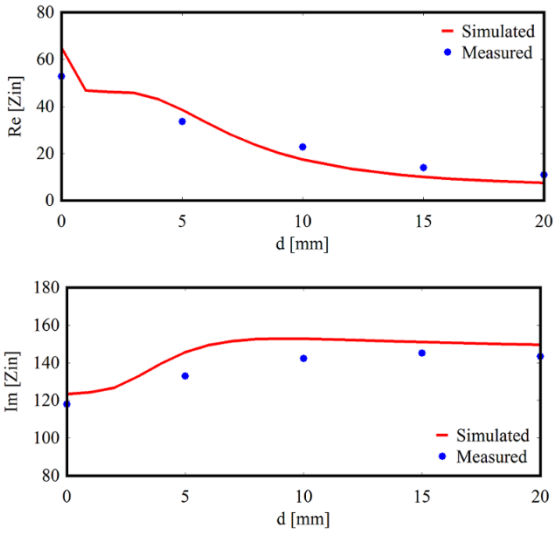

Figure 16. Simulated and measured input impedance of the NSSP-SME antenna in Fig. 13 (right).

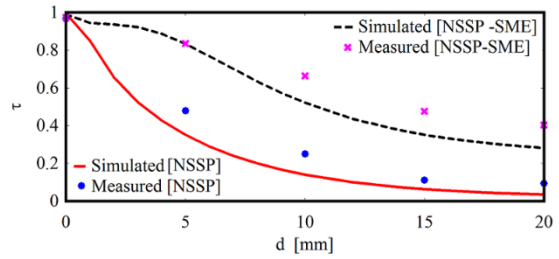

Figure 17. Simulated and measured power transmission coefficient τ of the NSSP and NSSP-SME antennas in Fig. 13.

In Fig. 17, the simulated and measured power transmission coefficient τ (normalized to Z_{chip} = 73-j113 Ω) is reported for both the NSSP and the NSSP-SME antennas. As expected, the NSSP-SME configuration provides higher values of τ when the antenna-body separation increases (measured τ is greater than 0.7 for a distance d less than 10 mm).

IV. Conclusion

Design guidelines have been presented to improve the robustness of ungrounded wearable antennas with respect to the antenna-body separation. A design criterion is achieved by an *a priori* analysis of the electric and magnetic energy densities distributions in the antenna near field region, leading to a suitable layout modification. Two different kinds of antennas have been analyzed. Firstly, lumped capacitors have been introduced in a solid-line resonant loop antenna to concentrate the electric energy far from the antenna borders, thus improving the insulating capability of the dielectric substrate. Then, we have applied our design criterion to an antenna consisting of an H-shaped slot placed onto a suspended patch. In this case, we have demonstrated, through both simulated and measured results, that a layout extension toward the antenna border where the electric energy density exhibits a maximum improves the antenna robustness to the human body proximity.

Although the present analysis is limited to only a couple of ungrounded antennas operating in the UHF RFID frequency range (860-960 MHz), it is the authors' opinion that design guidelines based on the electric and magnetic energy density distributions in the antenna near field region may help to avoid time-consuming brute-force optimization procedures in the context of the ungrounded wearable antenna design. Moreover, the proposed energy-based criterion is frequency independent, and can be employed for the design of ungrounded antennas operating in the whole UHF frequency range (300 MHz – 3 GHz), provided that a suitable modification of the antenna layout is able to confine the electric energy density far from the antenna border.

ACKNOWLEDGMENT

The authors thank Andrea Saba and Pasqualino Marongiu for their support in performing experimental measurements.

REFERENCES

[1] P. Nepa and H. Rogier, "Wearable antennas for off-body radio links at VHF and UHF bands (below 1 GHz): challenges, state-of-the-art and future trends," *IEEE Ant. Propag. Magaz.*, vol. 57, no. 5, 2015.

[2] P.S. Hall, Y. Hao, V.I. Nechayev, A. Alomainy, C.C. Constantinou, C. Parini, M.R. Kamarudin, T.Z. Salim, D.T.M. Heel, R. Dubrovka, A.S. Owadall, W. Song, A.A. Serra, P. Nepa, M. Gallo and M. Bozzetti, "Antennas and Propagation for On-Body Communication Systems", *IEEE Antennas Prop. Magaz.*, vol. 49, no. 3, pp. 41–58, 2007.

[3] A. Serra, P. Nepa, and G. Manara, "A wearable two-antenna system on a life jacket for Cospas-Sarsat Personal Locator Beacons," *IEEE Trans. Antennas Propag.*, vol. 60, no. 2, part II, pp. 1035-1042, 2012.

[4] P. Nepa and G. Manara, "On the Stochastic Characterization of Wearable Antennas," *PIERS 2013*, Stockholm, Sweden, Aug, 2013.

[5] A. Baroni, P. Nepa and H. Rogier, "Wearable self-tuning antenna for emergency rescue operations", *IET Microwaves, Antennas & Propag. Microwaves*, vol. 10, no. 10, pp. 173-183, 2016.

[6] A. Michel, K. Karathanasis, P. Nepa and J.L. Volakis, "Accuracy of a Multi-probe Conformal Sensor in Estimating the Dielectric Constant in Deep Biological Tissues," *IEEE Sensor Journal*, vol. 15, no.9, pp. 5217-5221, 2015.

[7] M. Manteghi and A.A.Y. Ibraheem, "On the study of the Near-Fields of Electric and Magnetic Small Antennas in Lossy Media," *IEEE Trans. Antennas Propag.*, vol. 62, no. 12, pp. 6491-6495, Dec. 2014.

[8] R. M. Makinen, T. Kellomaki, "Body effects on thin single-layer slot, self-complementary, and wire antennas," *IEEE Trans. Antennas Propag*, vol. 82, no. 1, pp. 385-392, Jan. 2014.

[9] G. A. Casula, A. Michel, P. Nepa, G. Montisci, and G. Mazzarella "Robustness of Wearable UHF-Band PIFAs to Human-Body Proximity", *IEEE Trans. Antennas Propag*., vol. 64, no. 5, May 2016.

[10] G. A. Casula, M. Altini, A. Michel and P. Nepa, "On the performance of low-profile antennas for wearable UHF-RFID tags," 1st URSI Atlantic Radio Science Conference, Gran Canaria, Spain, 2015

[11] M. Altini, G.A. Casula, G. Mazzarella, and P. Nepa, "Numerical investigation on the tolerance of wearable UHF-RFID tags to human body coupling", *IEEE Antennas and Propagation Symposium*, Vancouver, BC, Canada, July 20-24, 2015.

[12] G. Marrocco , "RFID antennas for the UHF remote monitoring of human subjects" , *IEEE Trans. Antennas Propag*., vol. 55, no. 6, pp. 1862 -1680, Jun. 2007.

[13] A. Kiourti, C. Lee and J. L. Volakis, "Fabrication of Textile Antennas and Circuits With 0.1 mm Precision," in *IEEE Antennas Wireless Propag. Lett*., vol. 15, pp. 151-153, 2016.

[14] R. Moro, S. Agneessens, H. Rogier, A. Dierck, and M. Bozzi, "Textile Microwave Components in Substrate Integrated Waveguide Technology," *IEEE Trans. Microwave Theory and Tech.*, vol. 63, no. 2, pp. 422 - 432, Feb. 2015.

[15] S. Agneessens, and H. Rogier, "Compact Half Diamond Dual-Band Textile HMSIW On-Body Antenna," *IEEE Trans. Antennas Propag*., vol. 62, no. 5, pp. 2374 - 2381, May 2007.

[16] X. Qing, C. K. Goh and Z. N. Chen, "A Broadband UHF Near-Field RFID Antenna," in *IEEE Trans. Antennas Propag*, vol. 58, no. 12, pp. 3829-3838, Dec. 2010.

[17] M. Dobkin, S. M. Weigand, and N. Iye, "Segmented Magnetic Antennas for Near-field UHF RFID", *Microwave Journal*, Jun. 2007.

[18] https://www.cst.com/products/cstmws

[19] V. T. Nguyen, C. W. Jung, "Impact of Dielectric Constant on Embedded Antenna Efficiency," *International Journal of Antennas and Propagation*, vol. 2014, Article ID 758139, 6 pages, 2014.

[20] G. Hartsgrove, A. Kraszewsky, and A. Surowiec, "Simulated biologicalmaterials for electromagnetic radiation absorption studies," *Bioelectromagnetics*, vol. 8, no. 4, pp. 29 - 36, 1987.

[21] S. Basat, S. Bhattacharya, A. Rida, S. Johnston, L. Yang, M. M. Tentzeris, and J. Laskar, "Fabrication and assembly of a Novel high-efficiency UHF RFID tag on flexible LCP substrate," in *Proc. Electronic Components and Technology Conf.*, 2006, pp. 1352–1355.

Giovanni Andrea Casula (M'04) was born in 1974. He received the Laurea degree (*summa cum laude*) in electronic engineering and Ph.D. degree in electronic engineering and computer science from the University di Cagliari, Cagliari, Italy, in 2000 and 2004, respectively.
Since March 2006 he is Assistant Professor of Electromagnetic at the Department of Electrical and Electronic Engineering of the University of Cagliari, teaching courses in electromagnetics and antenna engineering. His current research interests are: synthesis, analysis and design of wire, patch and slot antennas; wearable antennas design and interaction with the human body; design of substrate integrated waveguides (SIW) slot antennas; microwave antennas design using genetic programming; periodic structures design (EBG and AMC) through evolutionary programming; printed Log-periodic Dipole Antennas (LPDA) design using innovative feeding techniques and inkjet printing; low-cost RFID Tag design in the UHF band. He is author or coauthor of 38 papers in international journals, serves as reviewer for several international journals, and is a member of the Italian Electromagnetic Society (SIEm).

Andrea Michel received the B.E.,M.E. *(summa cum laude)*, and Ph.D. degrees in telecommunications engineering from the University of Pisa, Pisa, Italy, in 2009, 2011, and 2015, respectively. In 2014, he was a Visiting Scholar with the ElectroScience Laboratory, The Ohio State University, Columbus, OH, USA. During this period, he has been involved in research on a theoretical analysis on the accuracy of a novel technique for deep tissue imaging. He is currently a Post-Doctoral Researcher in Applied Electromagnetism with the Microwave and Radiation Laboratory, Department of Information Engineering, University of Pisa. His current research topics focus on the design of integrated antenna for communication systems and planar antennas for near field UHF–RFID readers. Dr. Michel was a recipient of the Young Scientist Award from the International Union of Radio Science, Commission B, Beijing, China, in 2014, and Gran Canaria, Canary Islands, in 2015.

Giorgio Montisci (M' 08) was born in 1972. He received the Laurea degree (*summa cum laude*) in electronic engineering and Ph.D. degree in electronic engineering and computer science from the University of Cagliari, Cagliari, Italy, in 1997 and 2000, respectively.
In November 2000, he became an Assistant Professor of electromagnetic fields, and since 2015 he is an Associate Professor at the Dipartimento di Ingegneria Elettrica ed Elettronica, University of Cagliari, where he teaches courses in electromagnetics and microwave engineering. He is author or coauthor about 50 papers in international journals and he is a member of the Editorial Board of International Journal of Antennas and Propagation and IET Microwaves Antennas & Propagation. His research activity is mainly focused on: analysis and design of waveguide slot arrays and SIW slot arrays, design and diagnostics of microwave components and antennas for radio astronomy and radar applications, wideband antennas for wireless applications, wearable antennas and sensors, RFID antennas, and printed antennas.

Paolo Nepa Paolo Nepa received the Laurea (Doctor) degree in electronics engineering *(summa cum laude)* from the University of Pisa, Italy, in 1990. Since 1990, he has been with the Department of Information Engineering, University of Pisa, where he is currently an Associate Professor. In 1998, he was with the Electro Science Laboratory (ESL), The Ohio State University (OSU), Columbus, OH, as a Visiting Scholar supported by a grant from the Italian National Research Council. At ESL, he was involved in research on efficient hybrid techniques for the analysis of large antenna arrays. He is also involved in the design of wideband and multiband antennas, mainly for base stations and mobile terminals of communication systems, as well as in the design of antennas optimized for near-field coupling and focusing. More recently, he is involved in channel characterization, wearable antenna design, and diversity scheme implementation, for body-centric communication systems. In the context of RFID systems, he is working on techniques and algorithms for UHF-tag localization and RFID-based smart shelves. His research interests include the extension of high-frequency techniques to electromagnetic scattering from material structures and its application to the development of radio propagation models for indoor and outdoor scenarios of wireless communication systems. Dr. Nepa received the Young Scientist Award from the International Union of Radio Science, Commission B, in 1998.

Giuseppe Valente received the Laurea degree in electronic engineering and Ph.D. degree in electronic engineering and computer science from the University di Cagliari, Cagliari, Italy, in 2007 and 2016. In 2009 he joined the National Institute for Astrophysics (INAF), Cagliari Astronomy Observatory, Cagliari, Italy, where he worked on the development of the receivers for Sardinia RadioTelescope (SRT). Since December 2016 he is a researcher at the Italian Space Agency. His research activity is mainly focused on electromagnetic design of passive and active devices for microwave and millimetre-wave receivers and instrumentation.